Build Simul (2018) 11: 663–676
https://doi.org/10.1007/s12273-018-0433-0

Daylighting and visual comfort of oriental sun responsive skins: A parametric analysis

Amir Tabadkani[1] (✉), Saeed Banihashemi[2], M. Reza Hosseini[3]

1. Department of Building and Architectural Engineering, Politecnico di Milano, Milano, Italy
2. School of Built Environment and Design, University of Canberra, Australia
3. School of Architecture and Built Environment, Deakin University, Australia

Abstract

This study reports on developing an innovative approach for the parametric analysis of daylighting and visual comfort, through a sun responsive shading system. The objective is estimating the annual daylight metrics and indoor glare discomfort. To this end, a review of the literature was carried out on three key concepts: smart facades, visual comfort, and parametric design, in order to develop a dynamic pattern of an oriental system for enhancing the daylight and visual performance. Afterwards, two geometrical components (Rosette modules and louvers) were applied, using Grasshopper plug-in for Rhino and daylighting plug-in DIVA, to investigate the indoor daylight quality through different geometrical and physical properties. This resulted in generating 6480 design variants, when several variables (rotation, distance to facade, time hours, transmittance properties and colors) that affect incoming daylight as well as visual comfort performance in a single office space in the hot-arid climate of Tehran were taken into account. Interactive correlations between the overall performance of kinetic patterns and visual performance were investigated through an optimization process. Analyses showed that the proposed approach is capable of significantly improving the shading flexibility to control daylight metrics and glare, via a full potential adaptive pattern to achieve the maximum visual comfort level based on LEEDv4 certificate.

Keywords

oriental skin,
daylight performance,
visual comfort,
algorithmic simulation,
parametric study,
optimization

Article History

Received: 30 August 2017
Revised: 8 January 2018
Accepted: 17 January 2018

1 Introduction

Daylighting is one of the most significant aesthetic and visual features of buildings, with significant impacts on the physiological and psychological needs of people who live and work in spaces where daylight is available (Pauley 2004). The potential positive effects of daylight on the indoor environment and occupants' comfort and well-being have been investigated since the ancient architectural typologies (Costa et al. 2013; World Bank 2014). And the evidence from research studies proves that daylighting contributes to the enhancement of workers' productivity in work places, as well as improving their physiological conditions (Hassanabadi et al. 2012).

Daylight, however, can cause visual discomfort like glare and unwanted reflections, and affect the thermal balance of rooms through overheating (Pauley 2004). Therefore, the most ambitious challenge for designers in an effective daylighting design is to keep the balance between maximizing daylight harvesting and risks control of potential discomfort (Banihashemi et al. 2012).

Inside buildings, where on average people spend 87% of their lives (Klepeis et al. 2001), conventional lighting is often supplied by electrical sources that are adequate for performing visual tasks, but lack the spectral combination and quality required to stimulate the circadian system (Konis 2017). Hence, daylighting, visual comfort indices (VCI), and their potentials on the applicability of emerging frameworks for investigating the development of a novel area-based daylighting during the building life span are of paramount importance.

In addition to VCI, the building envelope acts as a separating element between the external and the internal climatic conditions. This function makes it the main focus of

E-mail: seyedamir.tabadkani@mail.polimi.it

Nomenclature

VC	visual comfort	Ts	specular transmission
DA	daylight autonomy (%)	sDA	spatial daylight autonomy: percentage of floor area receiving more than 300 lx in occupied hours (%)
$DA_{average}$	daylight autonomy density ratio		
VCI	visual comfort indices		
WWR	window to wall ratio (%)	ASE	annual sun exposure: percentage of a floor area receiving 1000 lx in occupied hours more than 250 annually (%)
UDI	useful daylight illuminance (lx)		
$UDI_{average}$	useful daylight illuminance density ratio		
DGP	daylight glare probability (%)	L_s	luminance of the source (cd/m^2)
RGB	RGB colors' reflectance	P_i	position index of the i-th glare source
Rs	specular reflectance	E_v	vertical illuminance (lx)
Sr	surface roughness	$\omega_{s,i}$	solid angle of the i-th glare source based on the viewing position of the observer (sr)
Td	diffuse transmission		

the dynamic approach and adaptive systems that reconfigure themselves to meet comfort metrics and users' needs in conceiving of an envelope that is multifunctional, responsive and active (Loonen et al. 2013; Favoino et al. 2016).

With the above in mind, and given that daylight is one of the most vital regulators of human circadian rhythms (Duffy and Czeisler 2009), empirical studies on parametric adaptation devices and the possibilities of maximizing the visual performance and its integration with buildings envelope are missing (Karanouh and Kerber 2015). Studies such as the one by López et al. (2015) have developed adaptive architectural envelopes as a result of biomimetic principles in architecture. There is also no shortage of studies on daylight simulation techniques. So some investigators have used a wide range of technologies to overcome the challenges associated with the different daylighting scenarios (Boyce et al. 2003; Duffy and Czeisler 2009; Karanouh and Kerber 2015; Lopez et al. 2015; Lavin and Fiorito 2017; Gunay et al. 2017). However, there is still much to be investigated on parametric shading, daylighting and visual comfort metrics through the use of computational and parametric simulations (Pesenti et al. 2015; Mahmoud and Elghazi 2016; Reinhart and Wienold 2011). The present study is an attempt to address this gap.

In this setting, the integration of daylighting with architectural practices is the desired solution to optimize visual comfort performance via translating scientific knowledge into actionable information that can be applied to upgrade the well-being of building occupants (Bellia et al. 2017; Narangerel et al. 2016). This synthesis must be accurate in order to obtain the proper quality and quantity of daylighting, and avoid excessive light. Accordingly, window to wall ratio (WWR) and shading devices are critical physical aspects to establish a harmonization between the solar passive strategies and building envelope components, to keep the balance between sufficient daylight and visual discomfort (Yun et al. 2017).

Therefore, to fill the identified gaps, the present study aims at constructing an innovative approach towards an acclimated skin pattern for an office space in Iran, in which annual daylighting and visual comfort (VC) performance are calculated through parametric modeling principles. The approach draws upon parametric design principles, where generative features are grounded in the sun responsive shading, validated through Leadership in Energy and Environmental Design (LEED v4) certification.

2 Background

As per the European standard EN 12665, VC is defined as a "subjective condition of visual well-being induced by the visual environment" (ECS 2011b). Reliable indices are needed in a design process for analyzing the quality of the visual environment. Although few review studies are available on visual comfort indices in the literature (Carlucci et al. 2015; Reinhart 2014; Rubiño et al. 1994), studies on the integration of responsive skin systems with visual comfort are nonexistent. Moreover, there is no general approach on methodologies and metrics to evaluate the current objectives in parallel. The sections that follow picture a landscape of now available research on the topic.

2.1 Visual comfort indices

The discourse of research on VC is dominated by studies on analyzing the presence of adequate amount of light where discomfort can be caused by either too low or too high level of light as glare (Konstantzos and Tzempelikos 2017). With this in mind, quantifying the amount of light can be grounded on the pragmatic factors below:

– Useful daylight illuminance (UDI); UDI is the annual percentage of illuminance values on the reference point within the comfortable range of 100–2000 lx. The upper bound represents the percentage of the time when an oversupply of daylight leads to visual discomfort, and the lower bound represents when there is the shortage of daylight (Carlucci et al. 2015).
– Daylight autonomy (DA); this is defined as the percentage of the occupied hours in a year when the minimum illuminance is provided with the sole daylight (Pesenti et al. 2015). In the literature, particularly in the European standard of EN 12464-1 (ECS 2011a), a reference value of 300 lx is recommended on the task area for a typical user (Tzempelikos and Athienitis 2007; Reinhart 2004; Reinhart et al. 2006).
– Continuous daylight autonomy (DA_{con}); an improvement method of DA proposed by Rogers (2006), in which the available amount of natural light is further calculated at a given point of a space during occupation hours.

In addition to UDI, DA and DA_{con} calculations, and in order to analyze daylight autonomy design precisely, daylighting is analyzed using two more codified metrics in LEED v4. These are spatial daylight autonomy (sDA) and annual sun exposure (ASE) metrics, which form a clear picture of daylight spaces and visual comfort ultimately (Carlucci et al. 2015). According to Illuminating Engineering Society of North America (IESNA 2012), sDA describes how much an interior environment receives sufficient daylight of 300 lx in more than 50% of its occupied hours (Pellegrino et al. 2017). Its main advantage over DA is that sDA returns a single value representing the whole analyzed area. In addition, with respect to ASE and DA, DA contains no upper limit on illumination level, therefore, ASE provides the balance as a proxy for direct sunlight, an indicator of potential illuminance problems where it should be less than 10% during occupied hours. It measures the percentage of floor area that receives at least 1000 lx for at least 250 occupied hours per year, which must not exceed 10% of floor area.

There are several aspects that influence the discomfort glare experienced by a person in a room, such as the field of view, background luminance, excessive daylight, and material reflectance (Bodart and Cauwerts 2017). Therefore, assessing the possible glare discomfort is relied on incoming daylight, in which as suggested in IES standard LM-83-12, direct sun exposure over 1000 lx enhances the glare risk for occupants (IESNA 2012). Furthermore, the data can be filtered by analyzing the period of time and view angle domain or just evaluating a total discomfort glare for all indoor view directions throughout the year on each test point. In this paper the major glare metric, daylight glare probability (DGP) by Wienold and Christoffersen (2006) is used, following Eq. (1):

$$\mathrm{DGP} = 5.87\times10^{-5}E_{\mathrm{v}} + 9.18\times10^{-5}\log_{10}2\left(1+\sum_{i=1}^{n}\frac{L_{\mathrm{s},i}\omega_{\mathrm{s},i}}{E_{\mathrm{v}}^{1.87}P_i^2}\right) + 0.16 \quad (1)$$

Based on Eq. (1), the comfort criteria of glare is proposed by four main domains as tabulated in Table 1.

Table 1 Glare comfort criteria (adapted from Wienold and Christoffersen (2006))

Daylight glare probability	Glare comfort
DGP < 0.35	Imperceptible glare
0.35 < DGP < 0.4	Perceptible glare
0.4 < DGP < 0.45	Disturbing glare
0.45 < DGP	Intolerable glare

2.2 Parametric design

As the theoretical point of departure for this study, parametric design is a computational method that can apply both generative and analytical approaches from the perspective of design explorations, and indicates a fundamental shift from design alternatives to design logic (Leach 2009). Therefore, computational attributes are applied to facilitate a wider search area for multiple views of the design space. On one side, there is the 3D model interface that displays the geometric configurations and on the other side, an editor allows the designer to encode the algorithmic process (Banihashemi et al. 2017). This automatic generation of a class of design solutions contains four mains steps (Gürsel Dino 2012):
– Start conditions and parameters (input);
– A generative mechanism (rules, algorithms, etc.);
– The act of generation of the variants (output);
– The selection of the best variant.

An integrated package of Grasshopper and Rhino is the most common solution to establish the parametric principles. Rhino is a 3D modelling software that authorizes the designer to link the geometry layout to its implicit parameters by a plugin called Grasshopper (Rutten 2013; Greenberg et al. 2013). This plugin allows the user to design a form, and provide numerical calculations based on an algorithmic approach, where the modeling format deploys a node-based editor in which data are processed by wire connectors. In addition, Grasshopper is capable of changing the parameters through the nodes to produce a wide range of specified design solutions, and illustrate them for designers.

3 Research design

To link the parametric design approach to building visual environment and energy performance, computational tools

can be used effectively to gather qualitative and quantitative aspects of architectural performance and optimizing a form once it is created.

As shown in Fig. 1, this research presents an algorithmic and parametric design process developed in Rhino/Grasshopper and DIVA-for-Grasshopper. The integration of these three tools was necessary for fulfilling the objectives of this study: Rhino as a modelling tool, Grasshopper as a parametric interface, and DIVA (design, iterate, validate, and adopt) for daylight analysis application (Ward 1994). Ladybug is further utilized as an environmental plug-in for inputting time zones and delivering sun position coordinates.

For organizing the research flow of this study, the possibilities and limitations of creating a responsive building skin are explored via a side-lit south-facing office space, located in Tehran; Iran as a case study and in three phases (Fig. 2). As illustrated in Fig. 2, three major phases of model parameters, performance criteria and simulation dataset constitute the research design flow of this study which are elaborately explained in the Sections 3.1, 3.2 and 3.3, respectively.

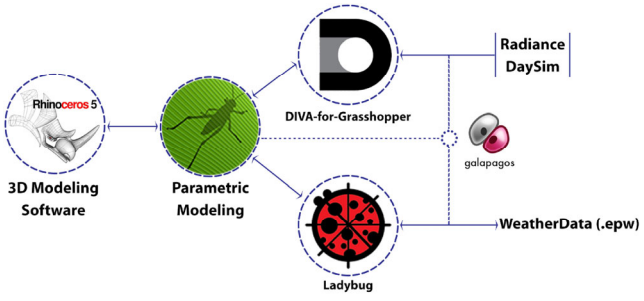

Fig. 1 Algorithmic integrated software workflow

As illustrated in Fig. 3, the first phase investigates converting an Islamic pattern where it has been used widely in different fields such as painting, mirrors or decorating, known as Islamic Star Patterns or Rosette (El ouaazizi et al. 2015; Abdullahi and Embi 2013), to a kinetic behavior of an oriental pattern, which is an acclimated shading device to control daylight uniformity via computational design tools of Grasshopper/Rhino.

In the second phase and in parallel with parameterized prototype, a list of critical visual comfort preferences that leads to lighting energy performance of the case study are developed through optimization the capabilities of Grasshopper. This phase is further progressed by DIVA (Jakubiec and Reinhart 2011), and is dedicated to daylight analysis via integration with Radiance and DAYSIM. As the third phase, and based on the input variables, the algorithm generates all the possible design solutions via an evolutionary solver function called Galapagos for further evaluation of the

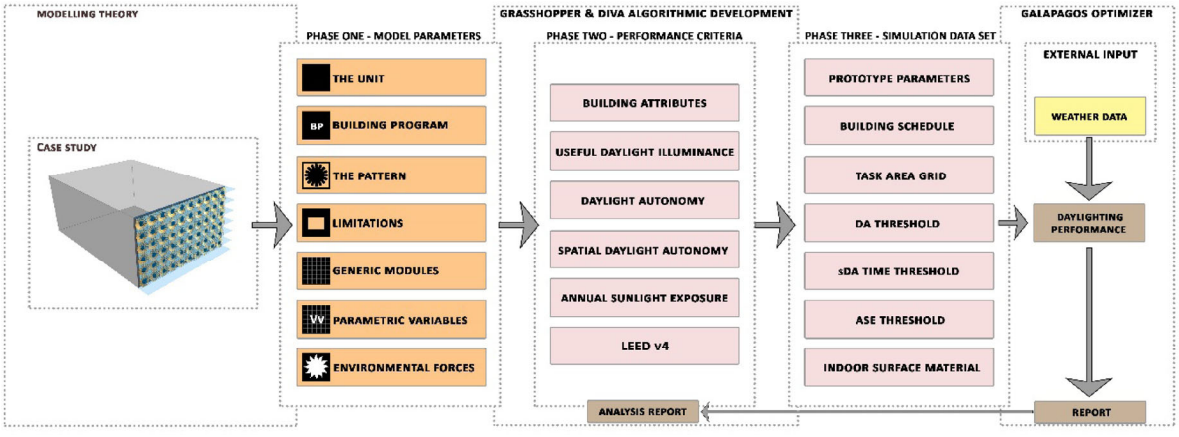

Fig. 2 Research design diagram

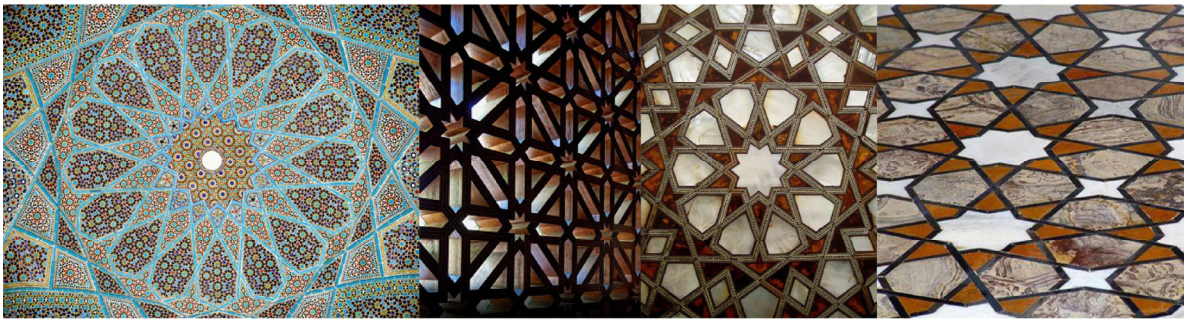

Fig. 3 Rosette pattern applications—from left to right: painting, wall, door, flooring

annual daylight metrics ($sDA_{300,\ 50\%}$ and $ASE_{1000,\ 10\%}$) based on an official building schedule. These phases are discussed next.

3.1 The first phase

In office-type environments, where occupants typically cannot freely adjust their position and have restricted visual comfort requirements, the building skin can provide sufficient indoor daylight using either smart facade orientations or automated shades (Reinhart 2014). Therefore, the process starts with considering the configurations of an oriental Rosette module that was applied to a completely glazed south face (WWR: 89.5%) of an office space with spatial dimensions of 5 m (width), 7 m (depth), and 3 m (height), as illustrated in Fig. 4. The measured space is 7 m in depth to give the opportunity to test the Oriental Skin efficiency.

Based on the responsive behavior of Rosette modules, where outer hexagonal cells of each module show the potential to deliver an interesting rate of rotation, an especially designated algorithm by the authors of this research, was linked to the Sun position, command in order to rotate Rosette outer hexagonal cells on each symmetrical axis, while sun position and its angle is changing. The sun position experimentation was constructed through a polar algorithm where it takes time parameters as the input variables and results in sun vectors directions as the output variables for evaluating the distance and angle to apply on Rosette rotation. The sun position diagram algorithm consists of two main steps, as depicted in Fig. 5, and discussed below:

1) Importing time parameters falling to three separate values (Fig. 5)
   a) Hour; that will be extracted from the minimum and maximum available total radiation during official working hours (8 AM to 6 PM),
   b) Day; this input is considered constant in whole simulations on 21st of each month,
   c) Month; it has been selected seasonally (March, June, September and December),
2) Extracting sun vectors directions via Ladybug to link the sun position determination with Rosette central cells

Furthermore, this step is completed with another algorithmic procedural instruction that is run by the parameters representing "Sliders" in Grasshopper to calculate rotational motion of Rosette modules, as explained below:

1) Implementing Rosette module on circular grid cells on the south face.
2) Importing a command to calculate rotational function of modules with respect to the sun position.
3) Measuring the distance between the Rosette central node and the Sun position resulted from Fig. 5.
4) Extracting maximum and minimum distances.
5) Selecting a rotation domain between 0 and 90 degrees for the Rosette hexagonal modules.
6) Remapping the distance values with rotation values, where the higher distance and angle figures of Rosette central cells overtake the higher rotation values.
7) Creating a symmetrical axis on each hexagonal cell.

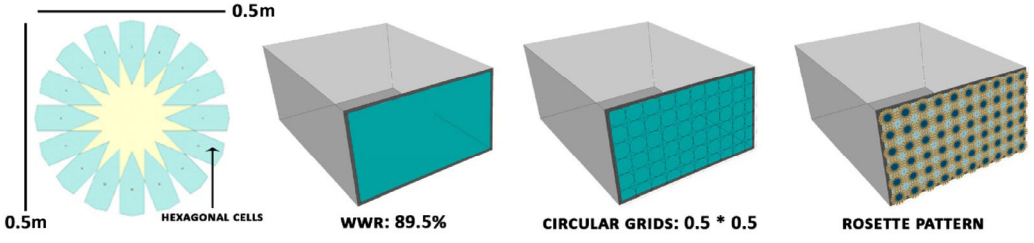

Fig. 4 Oriental Rosette modules

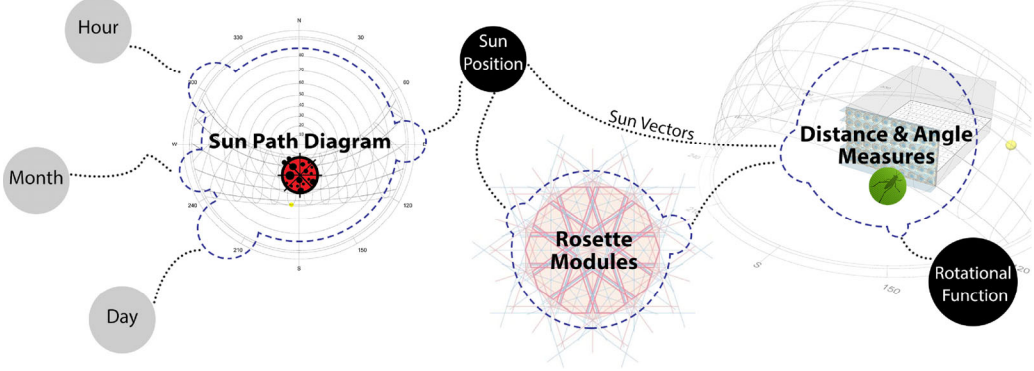

Fig. 5 Sun position to kinetic Rosette modules process

8) Applying remapped rotational values as angle degrees to manipulate rotation of individual Rosette modules.

Since the module is defined by adjustable parameters, changing the numerical values associated with each parameter can result in different shape rotations (Fig. 6). Figure 6 illustrates the different states of the modules between the unresponsive and responsive states. Figure 6(a) depicts the static Rosette modules, while Fig. 6(b) shows the responsive modules rotating from 0° to 90°. In line with Rosette modules for delivering sufficient uniform indirect daylight into the room, horizontal shade louvers were deployed among Rosette modules to control excessive unwanted daylight.

In addition to the different skin configurations and Rosette rotations, there is a transformation based on the following measures: (1) Rosette grid distance to the facade surface (a numerical range between 10 and 50 centimeters), and (2) horizontal louver depth (a numerical range between 50 and 100 centimeters), in which it justifies maximum Rosette distance value is the minimum louver depth, while the possibility of having the Rosette modules beyond the louvers is zero.

Although the geometry of the skin is a significant element in the overall daylight performance of a building, such geometric transformations contribute to the superior conformity to the visual comfort indices in the second phase.

3.2 The second phase

The second phase is primarily allocated to analyzing the influence of the kinetic system on the adaptability of facade. It should be noted that the focus of kinetics here is on the external features such as motions and fabrication of the skin to control internal illuminance. To accomplish this phase, DIVA-for-Grasshopper was used to explore the daylighting performance of each skin configuration and physical properties to meet visual comfort and LEED v4 metrics. DIVA-for-Grasshopper provides the advanced shading mode as the climatic metrics and it changes the parameters according to the user's threshold illuminance setting. The designer allows some skin layers to be controlled automatically, according to the amount of the light on a defined grid-based task area presumably with 80 centimeters height in this research, as illustrated in Fig. 7.

As illustrated in Fig. 7, the mock-up room has a double skin facade with a WWR value of around 90%. The louvers have also been set up on the ground to evaluate how louvers can block the sunlight and interact with Rosette modules to reflect to the interior spaces. This was deemed to allow for a clearer focus on the analysis of sDA, ASE and glare parameters in this study. At this stage, the fabrication properties of the model play a significant role in daylighting

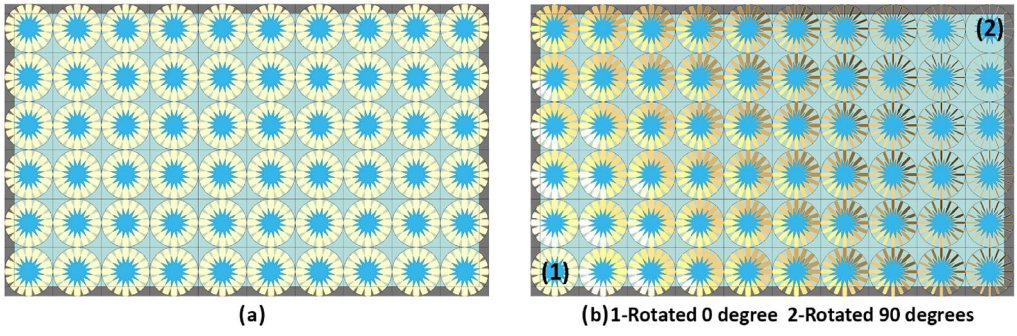

Fig. 6 (a) Rosette modules before being responsive; (b) rotation of Rosette modules (0–90 degrees)

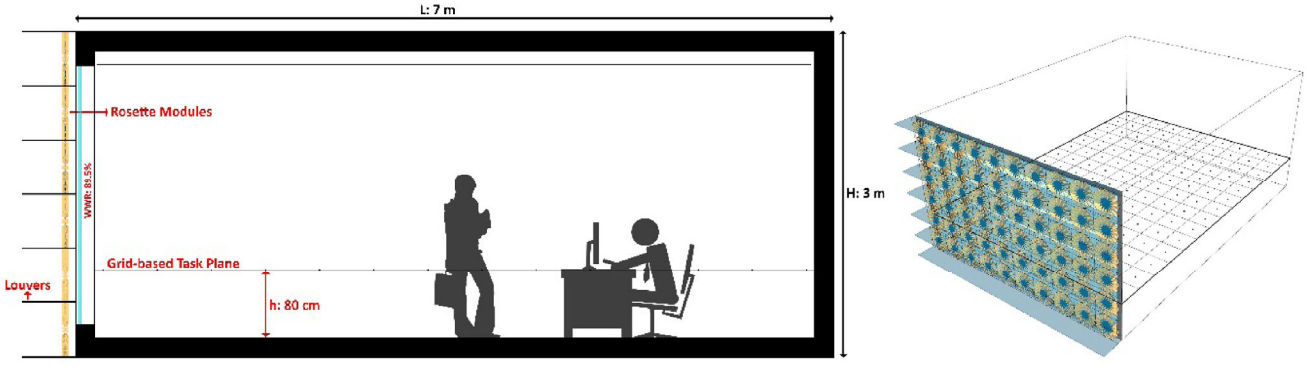

Fig. 7 Skin configuration and grid-based task area

performance that could result in visual comfort or discomfort. There are two types of assigned physical properties in this case study; (1) generic radiance materials including outside ground, interior ceiling, walls and floor; (2) customized glazing and radiance materials applied to south-faced glass and skin prototype.

DIVA radiance material library was used for defining generic radiance materials, in which they have the following requirements:

– Interior wall reflectance: 50%;
– Interior ceiling reflectance: 80%;
– Interior floor reflectance: 20%;
– Outside ground reflectance: 10%.

Customized radiance parameters were set by the same scene description format that is a combination of individual primitives or building components. All the scene primitives have the formats as tabulated in Table 2.

Eventually, in order to study the effectiveness of radiance material properties that were assigned to the Rosette modules and horizontal louvers, the following inputs were integrated into the algorithmic development:

1) Importing radiance parameters for the selected primitive types (plastic, metal and translucent);
2) Checking the radiance definition outputs;
3) Integrating radiance material definitions as variables for Rosette and Louvers as Scene Objects.

Moreover, since the south-faced glazed surface has a vital impact on permitting the natural light into the space depth, three different glass materials for glazing were proposed as input variables in DIVA simulations:

(1) Double pane-low emissivity with 65% visible light transmittance;
(2) Double pane-clear with 80% visible light transmittance;
(3) Single pane with 88% visible light transmittance.

After setting the fabrication radiance properties, the algorithm was synchronized to be imported into annually climatic daylight components in DIVA to compute VC indices, while it accepts the following requirements as shown in Fig. 8:

1) Importing customized scene objects and their specific Radiance material properties;

Table 2 Scene primitive features (adapted from Jacobs (2012))

Material code	Modifier	RAD type	Material description	Measures
			RGB reflectance (RGB)	RGB: black (0) to white (1)
0	Void [1]	Translucent	Specular reflectance (Rs)	Rs: a<0.1, b>0.9 [2]
1	Void	Plastic	Surface roughness (Sr)	Sr: almost zero
2	Void	Metal	Diffuse transmission (Td)	Td: fraction transmitted diffusely in a scattering fashion
			Specular transmission (Ts)	Ts: fraction transmitted as a beam

[1] *void* is used in the definitions because the primitive does not need to be modified by any other primitive.

[2] *a* is for plastic and translucent; *b* is for metal.

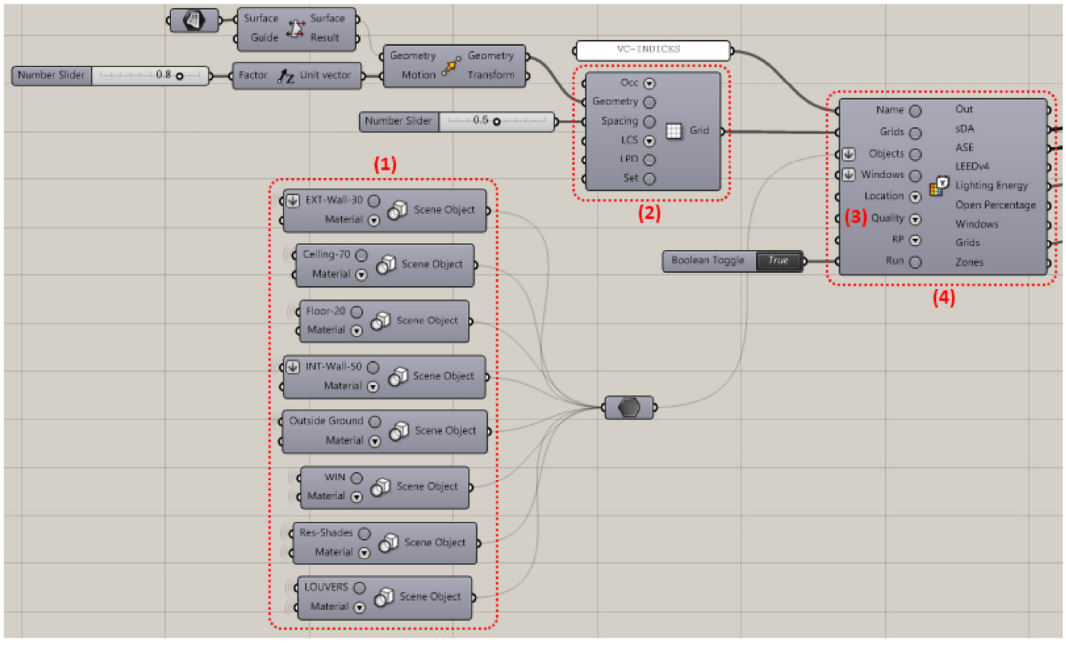

Fig. 8 Annually climatic daylight simulation in DIVA

2) Applying grid-based task plane with 80 cm height;
3) Defining radiance rendering quality settings in daylighting simulation;
4) Running annually climatic daylight simulation and extracting illuminance indices for VC analysis.

In fact, Fig. 8 demonstrates how scene objects and the relevant material properties are parametrized and linked with VC indices to the grid task layout and its configurations.

As evidenced in Fig. 9, the parametric model provides a constant feedback on the explorations of the proposed scenarios of the skin prototype by setting thresholds for the illuminance indices, while the annually climatic daylight simulation converts possible configurations into numerical values to measure the visual comfort based on LEED v4 (USGBC 2015) metrics. In addition, the main driving parameters are kinetic Rosette pattern based on the sun angle, the horizontal louvers, the radiance material specifications, and the motion scenarios as applied in DIVA/Grasshopper algorithmic process, as depicted in Fig. 9. The design objectives are focused on the five elements of kinetic skin, allowing for sufficient daylight, maximizing sDA, minimizing ASE, and ticking for LEEDv4 certificate. Rotation motion, distance to facade and radiance material constitute the model driving parameters of Rosette modules. Glass material, louver material and louver translation motion are the factors of the model driving parameters. In the next category, the building layout is represented via the glazing ration, task area height and space width, length and height. This category is also presented with the internal wall, ceiling and floor reflectance and the external ground reflectance parameters. In the end, time parameters of hour, day and month indicate the time liner of rotation of the louver and Rosette modules in this study.

3.3 The third phase

Analyzing and simulating smart building facades, and the dynamic test of their daylighting performance are proven challenging in the parametric design context. The third phase covers the analysis of the developed kinetic skins in applying the angular transformations in response to the dynamic daylighting and search for an optimal solution amongst. As illustrated in Fig. 10, designers are given a chance to explore the given VC dataset and select a design alternative by providing an opportunity to improve their selected design through the performance criteria parameters.

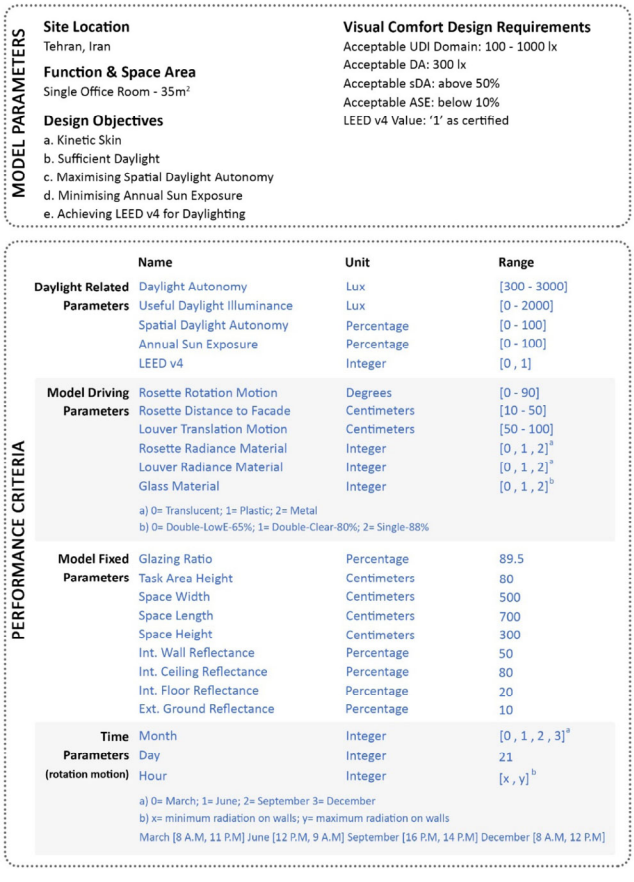

Fig. 9 Model parameters and performance criteria of the procedures towards simulation

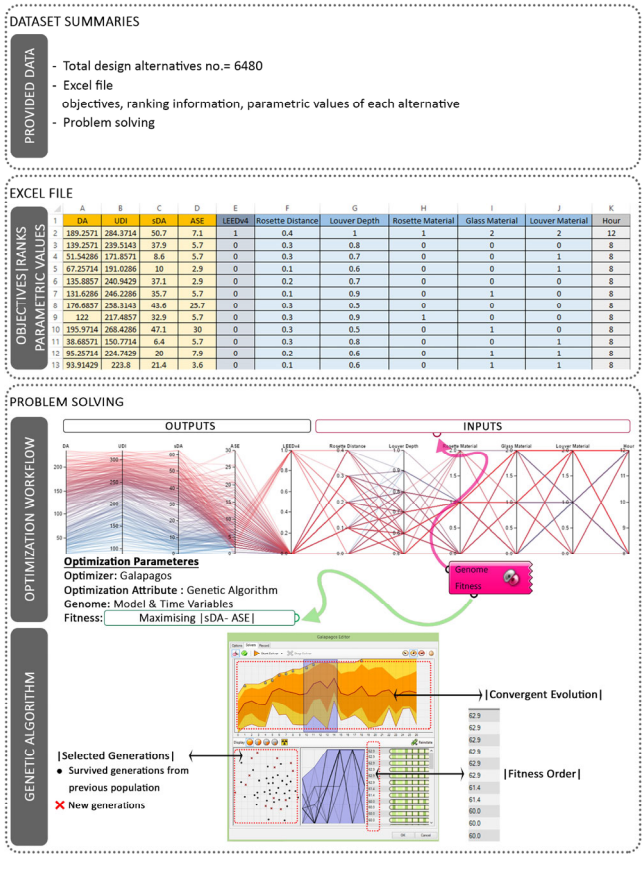

Fig. 10 Dataset summary of performance criteria

For the optimization stage and based on the list of parameters presented in Fig. 9 including the daylight, model driving, model fixed and time parameters, 6480 annual simulation runs were carried out using evolutionary algorithms of Galapagos as illustrated in Fig. 10. Galapagos is a tool included in Grasshopper (Rutten 2013), which applies the principles of genetic algorithm to converge the dataset into an optimum outcome. Once new generations have been simulated in this platform, the best alternatives are kept, based on the defined fitness function until their offspring gets closer to a convergent trend in the peak values. Hence, as depicted in Fig. 10, Galapagos takes the model and time variables as inputs to maximize sDA and ASE through the fitness function to generate the outputs constrained to the requirements of LEED v4.

4 Major findings

Daylight simulations were conducted by inputting annual weather data of Tehran where a daylighting model of an office room was developed. Fabric properties of the model are shown in Fig. 10, in which it recalls the reflectance measurements for a generic envelope, skin prototype and physical transformations based on the time intervals.

Following this process, all generations were exported to the Microsoft Excel spreadsheets to illustrate the possible solutions via Design Explorer application, an open source tool for exploring multi-objective parametric studies (Thornton Tomasetti 2017). As expected, all the input parameters turned out to have a significant effect on the daylighting quality across different reference points. Hence, in the baseline model, the room has no protection from sunlight, and as such, the points closer to the window present worse results than that of ones further away. Evidently, the inclusion of an external responsive skin prototype plays a remarkable role on improving visual comfort metrics of ASE, sDA and DA as daylighting quality for different modules.

The best possible adjustments were found by reaching the balance between ASE and sDA, where the algorithmic procedure aims to maximize the $sDA_{300,50\%}$ value while minimizing the effect of $ASE_{1000,10\%}$ to avoid a direct sun exposure inside the room.

The parametric analysis conducted in DIVA generated outcomes for the internal daylighting conditions, and as a consequence, for the visual comfort demand for occupants based on the daylight amount and quality that were assumed.

The first section of the result analysis is focused on the influence that different physical transformations along with their assigned radiance materials have on the internal daylight quantity, spatial distribution and sun exposure. Results were presented via a Design Explorer, which was specifically developed to represent the considerable number of daylighting results obtained from the parametric study.

The graphs were designed in order to account for all the variables influencing the performance: time zones (two hours), Rosette module distance to the south-faced surface, louver depth (along y-axis), Rosette rotation from 0 to 90 degrees (along with each hexagonal symmetric axis), louver transformation from 0.5 to 1 meter, radiance materials (3 types) and glass materials (3 types). Four separated graphs were reported to account for different months and time zones that are accessible via online links[1], where the generated values of March are only depicted here, as the representative of the rest, in Fig. 11. This figure exemplifies the Design Explorer application on the developed dataset of design solutions for March. It is represented in three main sets of time hours, Rosette and louver distances to the facade and fabrication material definitions. Through changing the markers of included parameters, the customized design generation can be reviewed and its daylighting performance can be assessed. The tool was used to point out which combinations of room features allow a certain daylighting performance criteria including; $DA_{300,\,lux}$ (average value of surface area, $DA_{average}$), $UDI_{100\text{-}1000,\,lux}$ (average value of surface area, $UDI_{average}$), $sDA_{300,\,50\%}$ and $ASE_{1000,\,10\%}$ that results in LEED v4 certification.

Following the parametric dataset obtained from Design Explorer, the series of LEED certified outputs were identified for each quarter that of March is presented in Table 3. For the sake of brevity, the remainder outputs are presented in Appendices (A, B and C) in the Electronic Supplementary Material (ESM) of the online version of this paper, in order to assess the effective coefficient of input variables. As illustrated in Table 3, in terms of materials, metal and plastic are the best choices for the louver and the Rosette. As for the the glass category, 80% of DBL has the dominance with 7 selections. The best time is varying between 8 and 11 a.m., while the louver depth and Rosette distance have wide ranges from 0.6 to 0.9 m and 0 to 0.2 m, respectively. Considering the reported inputs, the sDA has been maximized up to 59.3% and ASE has recorded the minimum of 0.7%. In overall, sDA ranges from 50% to 59.3% and ASE is constrained to the threshold of 0.7 to 8.6%. Table 3 indicates that there are 11 sets of inputs and outputs, which could meet the LEED v4 criteria, considered as the optimum choices.

Basically, the optimal generations for meeting the requirements are quite likely to be obtained in both time hours. Therefore, Rosette distance and louver depth have different impacts on indoor daylighting performance. By increasing the gap between Rosette and facade, sDA and ASE can be both enhanced while extruding the horizontal

[1] March: https://goo.gl/S5PLQb; June: https://goo.gl/qXJy4d; September: https://goo.gl/vUqCMW; December: https://goo.gl/5jGf8k .

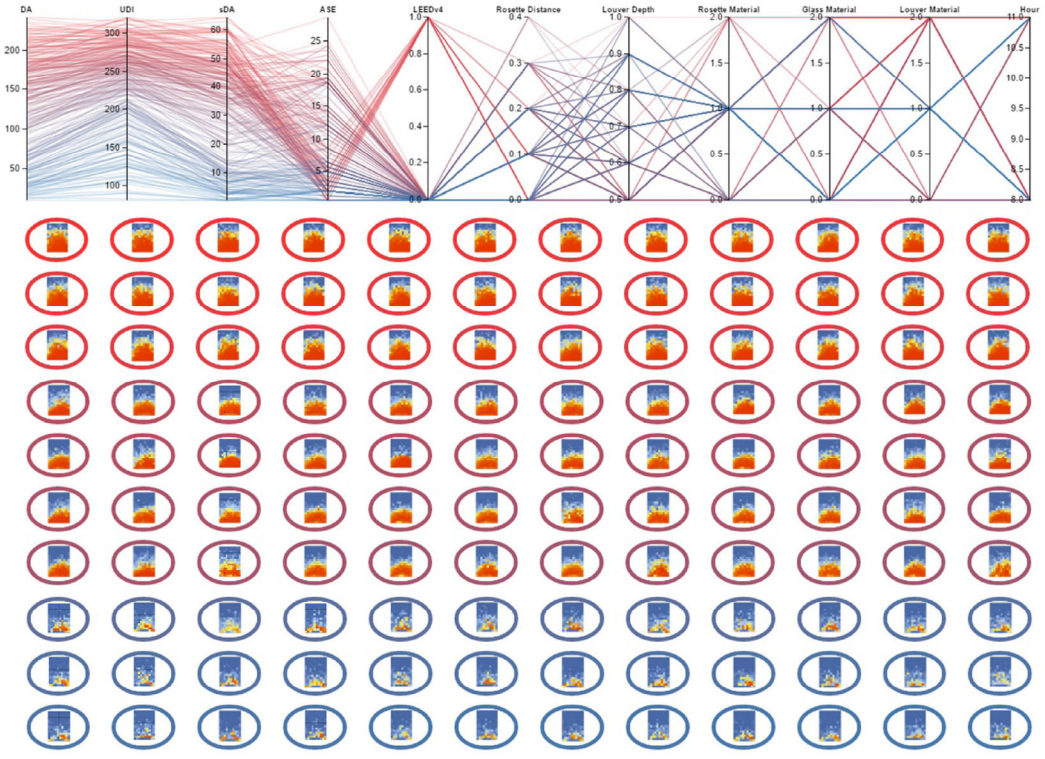

Fig. 11 Selected generations based on $DA_{average}$ of March

Table 3 Selected optimums for March

$DA_{average}$	$UDI_{average}$	sDA (%)	ASE (%)	LEEDv4	Rosette distance (m)	Louver depth (m)	Rosette material	Glass material	Louver material	Hour
196.05	302.22	52.1	5	✓	0	0.6	Plastic	DBL-65%	Metal	11
189.42	271.82	50	0.7	✓	0	0.9	Plastic	DBL-80%	Metal	8
205.08	319.14	55	8.6	✓	0.2	0.6	Plastic	DBL-80%	Metal	11
204.85	288.22	51.4	1.4	✓	0	0.8	Plastic	SGL-88%	Metal	8
195.37	284.6	50.7	3.6	✓	0	0.7	Plastic	DBL-80%	Metal	8
195.6	282.7	51.4	2.1	✓	0.1	0.9	Plastic	DBL-80%	Metal	11
203.02	290.28	54.3	3.6	✓	0	0.6	Plastic	DBL-80%	Metal	8
203.02	290.28	54.3	3.6	✓	0	0.6	Metal	DBL-80%	Metal	8
197.94	275.28	50	2.9	✓	0.1	0.8	Plastic	SGL-88%	Metal	8
219.51	304.42	59.3	5	✓	0	0.6	Plastic	DBL-80%	Metal	11

louvers can minimize them. Thus, the optimum design models are obtained for all time hours when Rosette distance reaches its minimum value as 10 cm and louver depth is 60 cm to achieve LEED certification in the meanwhile of delivering the desired visual comfort and daylight amount.

As depicted in Fig. 12, the attached louvers can minimize the direct sunlight significantly as compared to a non-shaded facade in selected time hours, while keeping required indoor daylight above 50% of floor area. louver and Rosette protection systems have both reduced effectively the sDA but the latter has acted far better in ASE minimization by around 40%–45%. Figure 12 approves that the sole implementation of the horizontal shading system as the louver protection mechanism could not create the LEED certified outputs. However, its effective integration with the responsive Rosette skin showed a progressive potential to deliver sufficient indoor daylight and prevent unwanted internal direct sun exposure. This achievement has resulted in certified design solutions based on the LEED v4 metric.

In the third set, the influences of different material definitions assigned to Rosette, louvers and the south-faced window are extracted and depicted in Fig. 13. Regarding

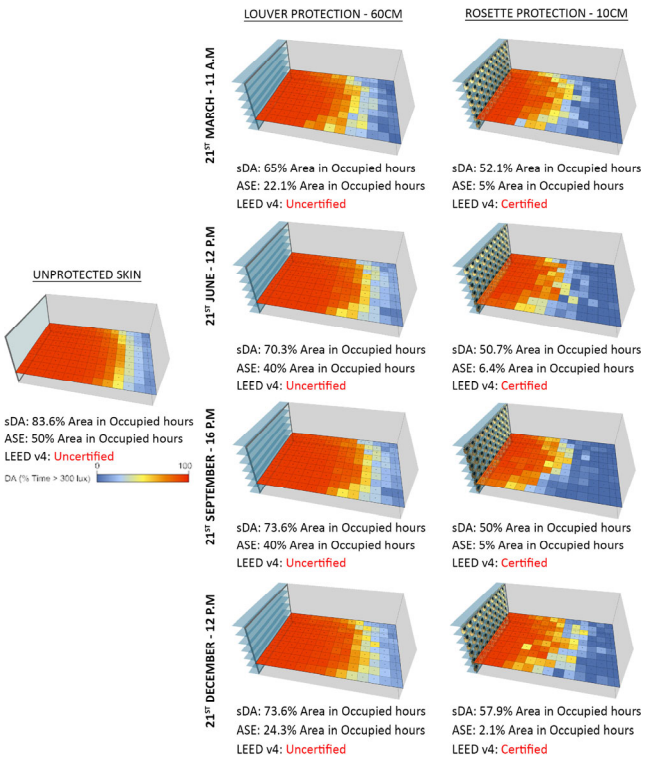

Fig. 12 The performance of unprotected skin vs. louver and Rosette protection

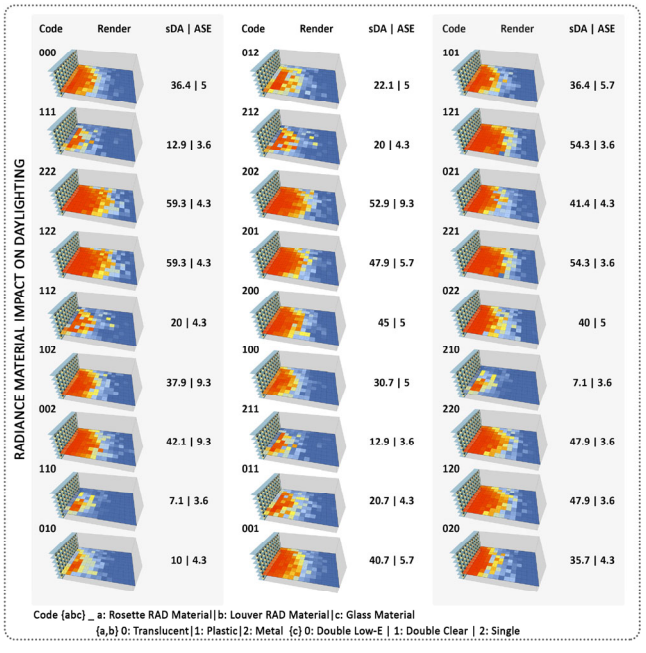

Fig. 13 Generated simulations based on the fabrication properties in March

responsive skin material, all three types show intangible difference between applying translucent, plastic or metal materials in enhancing $sDA_{300,\,50\%}$, and minimizing $ASE_{1000,\,10\%}$. Metal plays a more significant role in providing the indoor visual comfort for horizontal louver fabrication settings. Also, the related optimum solutions are simulated when double-clear with 80% transmissibility and single-glazed with 88% transmissibility are applied on the glass. In general, it can be stated that Lover material and louver depth have more significant effects on sDA and ASE outputs. Likewise, the possible generations based on different material definitions of plastic, glass and metal are visualized in Fig. 13 for assisting designers and researchers with their function in daylighting comfort. Fabrication selection for each component revealed that optimum design solutions are obtained when metal louver is assigned for the skin to minimize direct sunlight horizontally. Though, plastic rosette modules play significant roles on (1) enhancing the daylight performance during working hours of the year, and (2) scattering the sun rays into indoor environment. Moreover, the facade glazing material proves a drastic change in sDA by facilitating a higher transmittance. It has, however, less influence on the incoming direct daylight. With this respect, double glazing and low-emissivity coating windows can be of top alternatives in order to prevent excessive heat gain or loss during the year (Hassanabadi and Banihashemi 2012; Banihashemi et al. 2015).

Furthermore, in order to control DGP, the sun angle can be recorded during working hours of 21st of March to assess the responsive behavior of the pattern in controlling the glare discomfort. It uses DIVA-for-Grasshopper simulation software, while annual daylight metrics ($sDA_{300,\,50\%}$ and $ASE_{1000,\,10\%}$) is recorded simultaneously once daylight reaches the test surface. However, based on previous optimum solutions, the fabrication material is considered Metal, Plastic and DBL-80% for louvers, Rosette modules and glass respectively in glare analysis. Figure 14 illustrates glare inability in a direct field of view towards outdoor for each hour from 8 a.m. to 5 p.m., where the skin can effectively

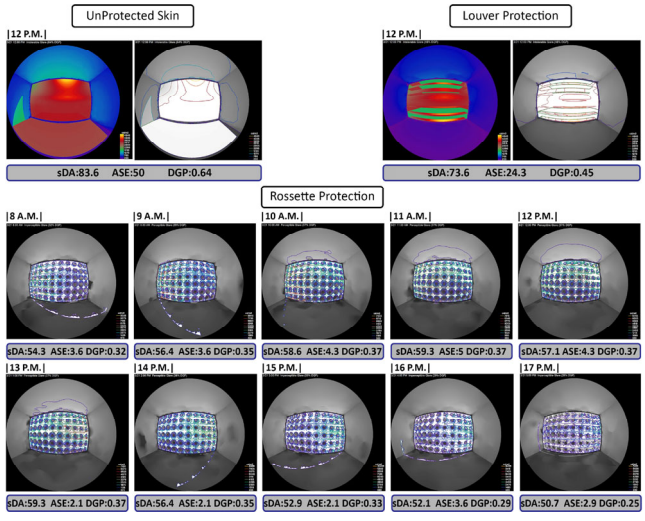

Fig. 14 DGP evaluation in March 21st

manage a balance between the incoming required daylight and glare discomfort. Consequently, implementing Rosette protection enhanced spatial daylight autonomy over 50% of the grid and minimized unwanted direct sun exposure below 5% in occupied hours. Moreover, the possibility of having disturbing glare is equal to zero and the user can experience visual comfort as Imperceptible Glare except only from 10 a.m. to 1 p.m., DGP is almost 0.37, the user can experience Perceptible Glare. At the same time (12 p.m.) comparing with unprotected skin and only louver protected facade, the glare discomfort is reduced from 0.67 and 0.45 respectively.

5 Conclusion

In order to evaluate visual comfort performance of an oriental responsive solar skin of a single south-faced office unit and to provide an adaptive shading system for occupants, a parametric analysis was conducted and employed in this study on an office case located in Tehran. The results showed an improvement in the performance of dynamic facades in comparison with the static systems, with an increase in sDA, while minimizing 10% for visual discomfort (ASE) and keeping an indoor glare-free environment for occupants. As a tried-and-tested procedure, the proposed method was found to be a workable solution in calculating the annual daylighting performance of a dynamic facade system and providing visual comfort. This is an important finding, as the aforementioned can assist in identifying the exact time of the year when the proposed screen requires adjustments based on the known sun vectors at specific hours.

As another finding, the geometrical properties and motions of two components, namely, Rosette modules and horizontal louvers were extracted from field measurements, and their fabric settings were applied in simulations. The optimization process increased the possibilities of achieving the maximum efficiency in the proposed solutions, where 6480 design variants were generated by a daylighting plug-in DIVA-for-Grasshopper. As a result, the proposed procedure was found effective in indoor improving the daylight uniformity given the correlation between geometrical attributes and orientations of screen positions considering visual comfort adjustment. With respect to the module responses, results revealed that rotation of Rosette patterns has a positive effect on distributing indoor illuminance while blocking direct sun exposure via installing horizontal louvers. In addition, it was found that plastic and metal materials are the best combination of the pattern configurations to achieve visual comfort requirements based on LEED v4 index. Accordingly, the optimized acclimated screen in this research has proven to achieve much better results in terms of useful daylight distribution compared with a base case with no shading.

Notwithstanding the above contributions and the novelty of findings, there are some limitations to be acknowledged. First, the findings should be treated with caution in direct application to real-life buildings, given that the data were collected through generating a fictitious office space. Second, the performance of the developed algorithm is open to enhancement to reach the minimum discomfort in the interim of maximizing the visual comfort. Third, the outside view and its technical and aesthetic paradigms were not investigated, being considered out of the realm of this research study. That was due to the level of subjectivity involved, which could compromise the validity of the analytical results and the modules setting of the kinetic system alike. Despite being limitations, these provide fertile grounds for research, warranting further investigation for validating the algorithm by using larger samples and from a wider typology of buildings covering institutional and industrial cases, to incorporate a range of design variables, and various parameters exposed to certain design constraints. Another area to be investigated pertains the role of setting louvers in different heights and combinations, with different kinetic mechanisms.

Electronic Supplementary Material (ESM): supplementary material is available in the online version of this article at https://doi.org/10.1007/s12273-018-0433-0.

References

Abdullahi Y, Embi MRB (2013). Evolution of Islamic geometric patterns. *Frontiers of Architectural Research*, 2: 243–251.

Banihashemi S, Hassanabadi MS, Sadeghifam AN (2012). Analysis of behavior of windows in terms of saving energy in extreme cold weather climes of Iran. *International Journal of Engineering and Technology*, 4: 676–679.

Banihashemi S, Golizadeh H, Hosseini MR, Shakouri M (2015). Climatic, parametric and non-parametric analysis of energy performance of double-glazed windows in different climates. *International Journal of Sustainable Built Environment*, 4: 307–322.

Banihashemi S, Tabadkani A, Hosseini MR (2017). Modular coordination-based generative algorithm to optimize construction waste. *Procedia Engineering*, 180: 631–639.

World Bank (2014). World Development Indicators 1960–2013. Washington DC: World Bank.

Bellia L, Fragliasso F, Stefanizzi E (2017). Daylit offices: A comparison between measured parameters assessing light quality and users' opinions. *Building and Environment*, 113: 92–106.

Bodart M, Cauwerts C (2017). Assessing daylight luminance values and daylight glare probability in scale models. *Building and Environment*, 113: 210–219.

Boyce P, Hunter C, Howlett O (2003). The benefits of daylight through windows. Rensselaer Polytechnic Institute.

Carlucci S, Causone F, De Rosa F, Pagliano L (2015). A review of indices for assessing visual comfort with a view to their use in optimization processes to support building integrated design. *Renewable and Sustainable Energy Reviews*, 47: 1016–1033.

Costa A, Keane MM, Torrens JI, Corry E (2013). Building operation and energy performance: Monitoring, analysis and optimisation toolkit. *Applied Energy*, 101: 310–316.

USGBC (2015). Leadership in Energy and Environmental Design (LEED). U.S. Green Building Council.

Duffy JF, Czeisler CA (2009). Effect of light on human circadian physiology. *Sleep Medicine Clinics*, 4: 165–177.

ECS (2011a.) EN 12464-1. Light and lighting—Lighting of work places—Indoor work places. Brussels: European Committee for Standardization.

ECS (2011b). EN 12665. Light and lighting—Basic terms and criteria for specifying lighting requirements. Brussels: European Committee for Standardization.

El ouaazizi A, Nasri A, Benslimane R (2015). A rotation symmetry group detection technique for the characterization of Islamic Rosette Patterns. *Pattern Recognition Letters*, 68: 111–117.

Favoino F, Fioritio F, Cannavale A, Ranzi G, Overend M (2016). Optimal control and performance of photovoltachromic switchable glazing for building integration in temperate climates. *Applied Energy*, 178: 943–961.

Greenberg D, Pratt K, Hencey B, Jones N, Schumann L, Dobbs J, Dong Z, Bosworth D, Walter B (2013). Sustain: An experimental test bed for building energy simulation. *Energy and Buildings*, 58: 44–57.

Gunay HB, O'Brien W, Beausoleil-Morrison I, Gilani S (2017). Development and implementation of an adaptive lighting and blinds control algorithm. *Building and Environment*, 113: 185–199.

Gürsel Dino İ (2012). Creative design exploration by parametric generative systems in architecture. *METU Journal of Faculty of the Architecture*, 29(1): 207–224.

Hassanabadi MS, Banihashemi S (2012). Developing an empirical predictive energy-rating model for windows by using Artificial Neural Network. *International Journal of Green Energy*, https://doi.org/10.1080/15435075.2012.738451.

Hassanabadi MS, Banihashemi S, Javaheri AR (2012). Analysis and comparison of impacts of design optimization approaches with occupant behavior on energy consumption reduction in residential buildings. *International Journal of Engineering and Technology*, 4: 680–683.

IESNA (2012). LM-83-12 IES. Spatial Daylight Autonomy (sDA) and Annual Sunlight Exposure (ASE). New York, NY: IESNA Lighting Measurement.

Jacobs A (2012). Radiance Cookbook. Available at http://www.radiance-online.org.

Jakubiec JA, Reinhart CF (2011). DIVA 2.0: Integrating daylight and thermal simulations using Rhinoceros 3D, Daysim and EnergyPlus. In: Proceedings of the 12th International IBPSA Building Simulation Conference, Sydney, Australia, pp. 2202–2209.

Karanouh A, Kerber E (2015). Innovations in dynamic architecture. *Journal of Facade Design and Engineering*, 3: 185–221.

Klepeis NE, Nelson WC, Ott WR, Robinson JP, Tsang AM, Switzer P, Behar JV, Hern SC, Engelmann WH (2001). The National Human Activity Pattern Survey (NHAPS): A resource for assessing exposure to environmental pollutants. *Journal of Exposure Science and Environmental Epidemiology*, 11: 231–252.

Konis K (2017). A novel circadian daylight metric for building design and evaluation. *Building and Environment*, 113: 22–38.

Konstantzos I, Tzempelikos A (2017). Daylight glare evaluation with the sun in the field of view through window shades. *Building and Environment*, 113: 65–77.

Lavin C, Fiorito F (2017). Optimization of an external perforated screen for improved daylighting and thermal performance of an office space. *Procedia Engineering*, 180: 571–581.

Leach N (2009). Digital morphogenesis. *Architectural Design*, 79: 32–37.

Loonen RCGM, Trčka M, Cóstola D, Hensen JLM (2013). Climate adaptive building shells: State-of-the-art and future challenges. *Renewable and Sustainable Energy Reviews*, 25: 483–493.

López M, Rubio R, Martín S, Croxford B, Jackson R (2015). Active materials for adaptive architectural envelopes based on plant adaptation principles. *Journal of Facade Design and Engineering*, 3: 27–38.

Mahmoud AHA, Elghazi Y (2016). Parametric-based designs for kinetic facades to optimize daylight performance: Comparing rotation and translation kinetic motion for hexagonal facade patterns. *Solar Energy*, 126: 111–127.

Narangerel A, Lee J-H, Stouffs R (2016). Daylighting Based Parametric Design Exploration of 3D Facade Patterns. In: Proceedings of the 34th eCAADe Conference, At Oulu, Finland,

Pauley SM (2004). Lighting for the human circadian clock: Recent research indicates that lighting has become a public health issue. *Medical Hypotheses*, 63: 588–596.

Pellegrino A, Cammarano S, Lo Verso VRM, Corrado V (2017). Impact of daylighting on total energy use in offices of varying architectural features in Italy: Results from a parametric study. *Building and Environment*, 113: 151–162.

Pesenti M, Masera G, Fiorito F (2015). Shaping an Origami shading device through visual and thermal simulations. *Energy Procedia*, 78: 346–351.

Reinhart CF (2004). Lightswitch-2002: A model for manual and automated control of electric lighting and blinds. *Solar Energy*, 77: 15–28.

Reinhart CF, Mardaljevic J, Rogers Z (2006). Dynamic daylight performance metrics for sustainable building design. *Leukos*, 3: 7–31.

Reinhart CF, Wienold J (2011). The daylighting dashboard—A simulation-based design analysis for daylit spaces. *Building and Environment*, 46: 386–396.

Reinhart CF (2014). Daylighting Handbook I: Fundamentals; Designing with the Sun.

Rogers Z (2006). Daylighting metric development using daylight autonomy calculations in the sensor placement optimization tool. Available at http://www. archenergy. com/SPOT/SPOT_Daylight% 20Autonomy% 20Report. pdf.

Rubiño M, Cruz A, Garcia JA, Hita E (1994). Discomfort glare indices: a comparative study. *Applied Optics*, 33: 8001–8008.

Rutten D (2013). Galapagos: On the logic and limitations of generic solvers. *Architectural Design*, 83: 132–135.

Thornton Tomasetti (2017). Design Explorer. Github. Available at http://tt-acm.github.io/DesignExplorer.

Tzempelikos A, Athienitis AK (2007). The impact of shading design and control on building cooling and lighting demand. *Solar Energy*, 81: 369–382.

Ward GJ (1994). The RADIANCE lighting simulation and rendering system. In: Proceedings of the 21st International ACM Conference on Computer Graphics and Interactive Techniques, Orlando, FL, USA, pp. 459–472.

Wienold J, Christoffersen J (2006). Evaluation methods and development of a new glare prediction model for daylight environments with the use of CCD cameras. *Energy and Buildings*, 38: 743–757.

Yun G, Park DY, Kim KS (2017). Appropriate activation threshold of the external blind for visual comfort and lighting energy saving in different climate conditions. *Building and Environment*, 113: 247–266.